Implementation of Tension-based Compact Necklace-type Haptic Device Achieving Widespread Transmission of Low-frequency Vibrations

Yusuke Yamazaki, Hironori Mitake, and Shoichi Hasegawa.

***Abstract*—The haptic sensation of low-frequency vibration plays a vital role in the music listening experience, but it can be enjoyed only in certain facilities and environments. Many haptic devices have been proposed to convey music audio-induced vibration for various situations. Such devices require powerful, low-frequency vibration output and transmission over a wide area. Making such devices small and user-friendly is difficult, hindering their popularity. To promote haptic devices for music listening, this paper describes a method for developing a practical device using motors and a thread and evaluates this method's effectiveness. The proposed necklace-type device is small (about 55×58×15 mm), lightweight (58.5 g), and easy to wear, making it suitable for use during everyday travel. In addition, it can transmit low-frequency (20 Hz) vibrations, whose amplitude exceeds airborne vibration in a nightclub, to a wide area across the chest and neck, with a total power consumption of approximately 2 W. Our proposed method will contribute to the development of practical and high-performance haptic devices for music listening.**

***Index Terms*—Haptic Display, Wearable Device, Music Haptics, Entertainment, Human–Computer Interaction.**

I. INTRODUCTION

Haptic sensations play a vital role in enhancing the experience of music, movies, and other entertainment. Such sensations occur due to vibrations transmitted through a solid structure, such as a floor or chair (structure-borne vibration), or to air pressure changes from the sound source acting directly on the entire body (airborne vibration). Examples of the latter include heavy bass from large sub-woofers in live-music venues, nightclubs, and cinemas; the explosion of fireworks; and the sounds of guns and bombs during military maneuvers. However, feeling such sensations is difficult in daily life because of difficulty creating sufficiently loud noises. To expand the situations in which the haptic component of music can be enjoyed, various vibration devices have been designed [1], [2], [3], [4], [5]. In this paper, we focus primarily on music listening, among other entertainment content.

Y. Yamazaki and S. Hasegawa are with the Department of Information and Communications Engineering, School of Engineering, Tokyo Institute of Technology, Japan, e-mail: {yus988, hase}@haselab.net

H. Mitake is with the Department of Frontier Media Science, School of Interdisciplinary Mathematical Sciences, Meiji University, Japan, e-mail: mitake@haselab.net

A. Requirements of haptic stimulation for music listening

Previous studies have shown that low-frequency vibration plays a vital role in music listening. Hove *et al.* found that simultaneously presenting subjects with the acoustic and low-frequency vibrations of music enhanced their sense of "groove" with the music [6]. In another study, Merchel *et al.* had subjects sit in a seated whole-body vibration device and evaluated the quality of their experience when listening to music with and without vibration based on audio signals [7]. Four genres of music were included in their experiment, and subjects mostly preferred pop music with strong frequency components below 20 Hz.

Vibrations should be received over a wide body area to improve the experience of audio-haptic music listening. Vibrotactile sensation exhibits a spatial summation effect, in which stimulating a larger area of skin lowers the detection threshold [8]. In our previous research [9], we conducted a questionnaire on participants' impression of experiencing such sensations. The subjects preferred music listening using our prototype (Fig. 1(c)), which used a thread to transmit vibration to a wide area, over a linear vibrator that transmitted vibration from a single point.

Here, we determine the specific amplitude of low-frequency vibration that should be transmitted to the body for optimal music enjoyment. In this paper, we assume a representative situation of music listening near the loudspeakers in a nightclub, a location that allows for pronounced haptic sensation. In nightclub music contexts, the acoustic pressure typically reaches 130 dB [10]. We also define "low frequency" as 20 Hz, which is widely considered the lower limit of the audible range in everyday circumstances. Takahashi *et al.* [11] showed that, when exposed to a 20-Hz sine wave with sound pressure levels (SPLs) of 100, 105, and 110 dB, vibration acceleration levels (VALs) of about 80, 85, and 90 dB, respectively, were measured on the subject's chest. Supposing that the VAL increases linearly with the SPL, we estimate that the VAL is 110 dB when the SPL is 130 dB. We converted VAL into $\mathrm{m/s^2}$ using the reference acceleration of $10^{-6}\mathrm{m/s^2}$, as stated in their paper. Therefore, the estimated value was 0.32 $\mathrm{m/s^2}$

at 20 Hz, and we define this value as a "reference amplitude" for the minimum amount of vibration required for enjoyment.

B. Problems with using existing vibration devices

Eccentric motors and linear vibrators, often used in general haptic devices, cannot be used within small haptic devices to transmit low-frequency vibrations over a wide area. Because these vibrators generate vibrations via the reaction force when moving an internal weight (Fig. 1(a)), the vibrator housing must be large enough to provide sufficient stroke volume (the internal weight's movement range) for useful vibrations. In addition, vibration transfer to the body takes place at the contact area with the housing, but the transmitted vibration amplitude is greatly damped by absorption into the skin [12]. Thus, transmitting substantial vibration requires a large vibrator or many small vibrators to increase the contact area, resulting in a larger haptic device.

C. Proposal

In our previous study, we proposed a vibration-generation mechanism using motors and a thread (Fig. 1(b)) that could transmit vibration over the user's torso [9]. We developed a prototype using this principle, with the thread wound around the user's torso (Fig. 1(c)), and evaluated its vibration transmission performance. This study demonstrated that, in principle, a small device could transmit low-frequency vibrations over a wide area. However, the prototype had several practical problems: the thin thread was troublesome to wind around the body and uncomfortable to wear, and the actuators consumed large amounts of electricity.

This paper proposes a design policy and implementation method for a necklace-type haptic device using our previously proposed driving principle and evaluates this method's effectiveness and the device's characteristics. The implemented device is practical for use during everyday travel, such as commuting, walking, and riding in a car or on public transport. It can transmit low-frequency vibration of greater amplitude than the airborne vibration transmitted by a loudspeaker playing a 130-dB sound.

II. Related Works

Much research has been conducted on the transmission of vibrations to a wide area of the human body to enhance the experience of entertainment content.

A. Haptic devices incorporating general vibrators

For example, previous studies proposed clothing- and chair-type haptic devices embedded with several small vibrators to directly stimulate any part of the body [2], [13], [14], [15], [16]. Because of their high spatial resolutions, these haptic devices are suitable for conveying collision sensations as well as complex information, such as distance or direction, by stimulating targeted areas of the body. However, small vibrators cannot produce vibrations with high amplitudes at low frequencies, as explained in Section I-B.

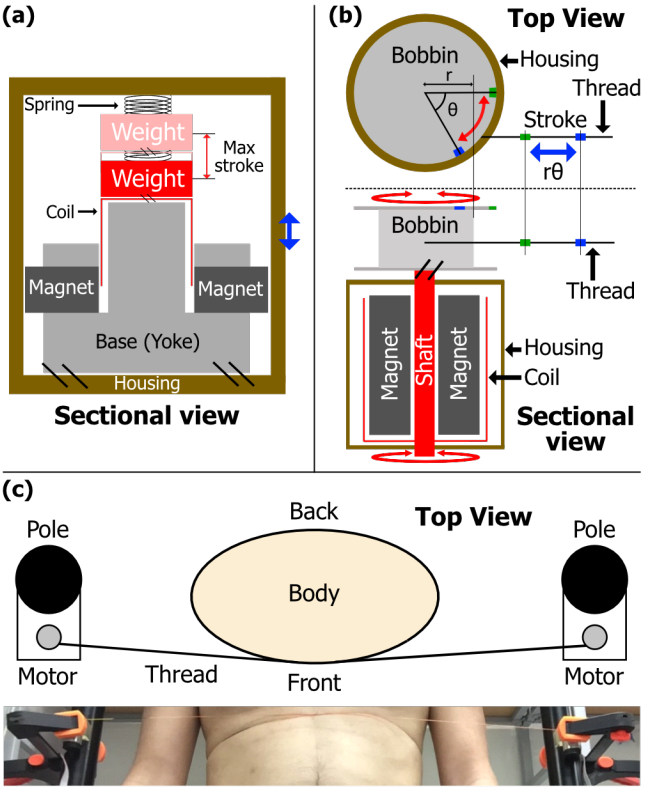

Fig. 1. Structure of (a) a linear vibrator and (b) our previously proposed driving principle. The red arrows indicate actuator movement, and the blue arrows indicate movement driven by the actuator. The blue and green dots in the top and sectional views in (b) indicate the maximum and minimum states of the output for a sinusoidal wave input. (c) Our previously proposed prototype using our driving principle.

Other haptic devices were developed with only a few large vibrators embedded in the back of a chair or a backpack [1], [3], [4], [17]. These devices have a low spatial resolution because they comprise only a few vibrators, but the large contact area of large vibrators contributes to each vibrator's extensive transmission of vibrations to the user's body. Large vibrators can also generate higher amplitudes of low-frequency vibrations than small vibrators because the mass and stroke of the internal weights are larger. This type of haptic device is thus suitable for generating low-frequency vibration derived from heavy bass when watching movies or listening to music, as mentioned in Section I. However, the size and weight of large vibrators make such devices less portable.

B. Transmitting vibrations through media

Some studies have proposed different approaches to efficiently transferring vibrations over a wider area. Sakuragi *et al.* [18] showed that placing a vibrator on the clavicle is an effective way to transmit vibrations through bone conduction In another study, Kurihara *et al.* [19] used granular Styrofoam as a medium for transmitting vibrations from a few small speakers, resulting in a method for distributing vibrations from a few small vibrators over a wide area. Withana *et al.* [20] applied properties of low-frequency acoustic wave propagation

in the human body to propose a low-resolution haptic interface. Their method, using a seated-type device, could direct haptic sensations to a specific body area, such as the stomach or head. These approaches involve transmission through an object, which requires simplifying the device and increasing the transmission range of a small number of vibrators. However, the vibrators used in these studies are still conventional and, hence, subject to the trade-off between an individual vibrator's size and its amplitude capacity for low-frequency output.

C. Generating vibrations using DC motors

Some researchers have proposed using a rotary direct current (DC) motor as an actuator. Yem *et al.* [21] showed that DC motors are capable of effectively driving low-frequency vibrations by harnessing the rotational motor's counter-torque and using the motor's rotor as the vibration mass. In similar research, Gourishetti *et al.* [22] proposed a relatively inexpensive method, a combination of a DC motor and a rigid stylus, for providing high-fidelity vibrotactile feedback comparable to that provided by a relatively expensive voice coil actuator. Additionally, Minamizawa *et al.* [23] and Nakamura *et al.* [24] used a rotational motor to drive a belt in contact with a fingertip. The rotational motion of the motor shaft, as the vibration source, was ultimately converted into a translational motion of the skin. This process achieved sizable skin displacement, effectively representing both static forces and low-frequency vibrations. The skin would detect artificially generated sensations, such as holding an object or feeling a collision or traction in a video game. However, these studies focused on the fingertips, a localized area, rather than directly addressing our aim to transmit vibrations over a wide area.

III. Design Policy

This paper proposes a design of a practical haptic device that can be used in the everyday travel situations mentioned in Section I-C and, using our previously proposed driving principle, can transmit low-frequency signals extensively to the user's body. The design requirements are as follows (details provided in the following subsections):

(1) The device can extensively transmit low-frequency vibration with an amplitude exceeding the "reference amplitude" defined in Section I-A.
(2) The device is portable, simple, and easy to put on; it can be used immediately in a public space.
(3) The device's audio noise is low enough such that other passengers are not bothered in public transport.
(4) The device's power consumption is low, extending battery life and reducing heat generation.

A. Transmitting low-frequency vibration extensively with a compact device

Our previous work [9] demonstrated that our original driving principle could transmit low-frequency vibrations effectively. The concept of the vibration generation is illustrated in Fig. 1(b). The bobbin is attached to the motor shaft, and one end of the thread is tied to the bobbin. The other end of the thread is wound around the bobbin several times and then rolled out of the housing. The thread is wound around the user's body and then similarly wound and fixed to another bobbin attached to a motor shaft located on the opposite side. Note that the material in contact with the body can be another material as long as the material is attached to the thread wound around the bobbin. When alternating current (AC) voltage is applied to the motor, the motor shaft rotates, causing the thread to move translationally. The angle of rotation (θ in Fig. 1(b)) has no limitation, so the limitation of vibration stroke ($r\theta$ in Fig. 1(b)) is determined by the length of thread wound by the motor. The moved thread deforms the contact area, transmitting vibration to the user. The advantage of this driving principle is that the vibration stroke can be long, and it is largely independent of the device size because the volume of the bobbin-wound thread and, hence, the bobbin, is small. The device can thus generate higher-amplitude, lower-frequency vibrations than conventional vibrators of similar size. In addition, the thread contacts a large portion of the user's body and transmits vibrations over a wide area without requiring several vibrators.

B. Shape of the device

To meet design requirement (2), we propose that the device be a necklace that users can easily wear without adjusting the length. Thus, the user would not need to adjust their clothing (e.g., by removing a jacket or loosening a belt, as when wearing a belt-type device), and the device could be quickly taken out of a pocket or bag and put on in a public space. The thread would contact the chest and wind around the neck, thus transmitting vibration over a wide area. We limited the device's weight to that of a lightweight smartphone since smartphone neck straps have been shown acceptable in the market. The drive circuit must be small enough to fit in a standard clothing pocket.

C. Suppressing audio noise

Given the device's usage contexts, its audio noise output should be acceptable to other passengers on public transport. The SPL in a running train or bus is 70–80 dBA [25], [26]. Because the SPL of a normal conversation with interlocutors one meter apart is about 60 dBA according to International Organization for Standardization (ISO) Standard No. 9921:2003, we aim to keep the SPL of device noise well below that. During development, we found that audio noise was mainly generated by friction from the moving parts and magnetostriction from the motor. Thus, we propose using a low-friction Teflon tube to guide the moving parts and a low-pass filter in the drive circuit.

D. Reducing power consumption

Reducing the device's power consumption is critical to improving its conveniences, such as longer usage time and lower heat generation. Our previously developed prototype applied a continuous DC voltage to the motors to generate a steady-state torque on the thread, entailing continuous power

consumption. A steady-state torque is likewise essential in necklace-type devices to maintain the thread tension that keeps the thread wound on the bobbin and achieves proper vibration output. Without this steady-state torque, the thread would unwind from the bobbin, allowing the motor shaft to wind the thread around itself through forward or reverse rotation. This would cause improper vibration output; for example, when an AC voltage of $\sin \omega t$ is input, the output vibration would be $|\sin \omega t|$, halving the amplitude and distorting the intended waveform. To reduce power consumption, we propose providing steady baseline tension to the bobbin using a rubber cord instead of applying a DC voltage.

IV. Implementation

This section describes implementations of (1) the vibration transmitter, (2) the steady tension mechanism, and (3) the drive circuit that satisfy the requirements listed in Section III. Fig. 2 shows the structure of the developed device, named the Hapbeat, and its components. The necklace component is about 55×58×15 mm, with a mass of 58.5 g, which is smaller and lighter than a lightweight smartphone.

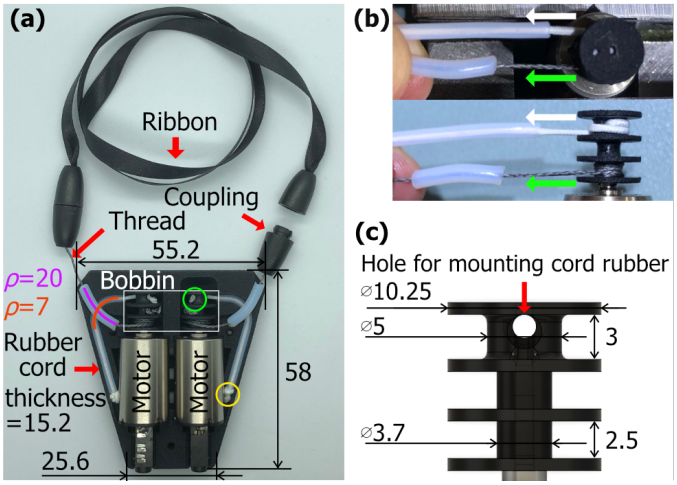

Fig. 2. (a) Components of the Hapbeat. All dimensions are in millimeters, where ρ is the curvature radius of the tube through which the thread (purple line) and the rubber (red line) run. (b) Tension direction. The green arrow indicates the direction of the tension applied to the bobbin when the thread is wound, and the white arrow indicates the tension caused by the rubber cord. (c) Dimensions of the bobbin (mm).

A. Vibration transmission component

The material of the vibration transmission component should be rigid enough to consistently transmit the alternating tension produced by the motor shaft rotation. We selected a thread made of ultra-high molecular weight polyethylene fiber (RUNCL PowerBraid, four strands, 95 lb per 0.50 mm). This thread can transmit vibrations directly to the body, but it is thin and uncomfortable to wear. Additionally, the part contacting the skin gets dirty from sweat and other factors, so separating it from the housing allows for easy cleaning. Thus, for the contact material, we selected a high-rigidity satin ribbon (6 mm wide, 100% polyester) that connects to the thread with a plastic coupling.

A thread guide is needed to reduce friction between the thread and housing and change the direction of the thread unwound from the bobbin (Fig. 2(a)). Friction between the guide and thread needs to be low to avoid additional audio noise, signal distortion, and damage to the thread. Therefore, we used a Teflon tube (Chukoh Chemical Industries, Ltd. PTFE tube, inner diameter of 1 mm, outer diameter of 3 mm) as a guide. To reduce friction, we minimized the curvature of the guide within the constraints of the small housing, as shown in Fig. 2(a).

A coreless motor was chosen to provide a low moment of inertia, allowing for quick repetitions of forward and reverse rotation to reproduce audio-like AC signals. The coreless motor used in the Hapbeat has the following characteristics: 3 V rated voltage, 1.1 Ω armature resistance, 1.92 W maximum output, 6.8 $\mathrm{mN \cdot m}$ stall torque, 10 ms mechanical time constant, 0.6 $\mathrm{g \cdot cm^2}$ rotor moment of inertia, and 110×10^3 $\mathrm{rad/s^2}$ angular acceleration.

B. Mechanism generating steady-state torque

We used a rubber cord (KawamuraSeichu Co. Ltd, elastic cord, 1 mm in diameter, white, natural rubber and rayon, 36 mm long), which combines thinness and a low Young's modulus, as the spring material to generate steady thread tension. One end of the rubber cord was fixed to the bobbin (green circle in Fig. 2(a)), and the other was fixed to the guide attached to the housing (yellow circle in Fig. 2(a)), thereby applying counter-torque when the thread was unwound from the bobbin (white arrows in Fig. 2(b)). We designed the bobbin to have four flanges to prevent the thread from being completely unwound when the Hapbeat is worn around the neck. The guide for the rubber cord is made of the same material as the thread guide (inner diameter of 1.5 mm, outer diameter of 2.5 mm).

C. Driver circuit design

The driver circuit should be battery-powered for portability and capable of driving the motor at the maximum effectual output with audio signal input. We adapted a single-cell lithium-ion battery (3.7 V) for the circuit to permit simple charging with a smartphone charger. A class-D amplifier IC (Diodes Incorporated, PAM8403) was used to amplify the input audio signal. However, a general audio amplifier IC alone cannot drive the motor (rated at 3 V, 1.1 Ω resistance) at the maximum effectual output (1.92 W) as the motor requires currents up to 1.93 A. Therefore, we constructed an H-bridge circuit by connecting the gate terminal of a field-effect transistor (Toshiba Electronic Devices & Storage Corporation, TPC8408) to the output of the amplifier IC. Additionally, to counter the audio noise described in Section III-C, we implemented a low-pass RC filter (C = 2.2 μF, R = 1 kΩ, cutoff frequency 72 Hz), which can easily be switched on and off with a slide switch. The schematics and frequency response results are shown in the appendix.

V. Evaluation

The following four experiments were conducted to evaluate how well the Hapbeat, as described in Sections III and IV,

satisfies the requirements outlined in Sections I and III. Sections V-A–V-B explain how we measured vibration transmitted from the Hapbeat to the user's body. We show that the Hapbeat maintains the performance of our previously proposed driving principle and transmits low-frequency vibration over a wide area that exceeds the reference amplitude criterion set in Section I-A. We also evaluate the fidelity of the transmitted vibration to the input signal from frequency components. Sections V-C–V-D show how we measured the power-saving effect of the steady tension mechanism implemented in Section IV-B and the effect of internal friction generated by this mechanism. In Section V-E, we assess the audio noise of the Hapbeat and the effect of a low-pass filter to determine whether the Hapbeat is appropriate for use on public transport. In Sections V-F–V-G, we measure the frequency response and response time of Hapbeat to inform potential users about the device.

A. *Vibration transmission measurement on subjects' body*

1) Subjects: The subjects were six men. Their heights, weights, body mass indexes (BMIs), and body fat percentages are listed in Table I. Their weights and body fat percentages were measured with a body composition meter (Tanita Corporation, innerScan Dual RD-802).

TABLE I
INFORMATION OF SUBJECTS

	sub-1	sub-2	sub-3	sub-4	sub-5	sub-6
Height (cm)	185	160	164	165	178	174
Weight (kg)	61.8	47.3	52.4	56.8	61.1	74.1
BMI (kg/m^2)	18.1	18.5	19.5	20.9	19.3	24.5
body-fat (%)	12.1	12.3	16.9	18.7	18.8	24.3

2) Measurement points: Measurements were taken in three different areas: chest, neck side, and nape, as shown in Fig. 3. To determine appropriate measurement points applicable to multiple subjects, we conducted a pilot experiment measuring transmitted vibration at the location marked by black and yellow dots in Fig. 3 with one subject (sub-6 in Table I). Those results were used to select the points marked by yellow dots in Fig. 3 for the following reasons:

Overall, we omitted the left side because the measurements on both sides were similar and tended to decay with distance from the ribbon and housing. First, in the chest area, we selected points near the ribbon where the vibration would be most intense, which we assumed to be important for perception. Second, we selected points on the clavicle because Sakuragi *et al.* showed that the clavicle provides an effective transmission channel [18]. Third, we chose a column perpendicular to the housing to observe the mixing of vibrations from the housing and the ribbon. Finally, we selected points 4 cm away from contact points A and C in Fig. 3 to observe the decay trends under different contact conditions. In the neck side and nape area, we selected the points near the ribbon for the same reasons as those for the chest and selected a central column to observe the damping trend.

3) Vibration signals and measurement: Input signals were supplied using a function generator (FeelTech, FY6600-30),

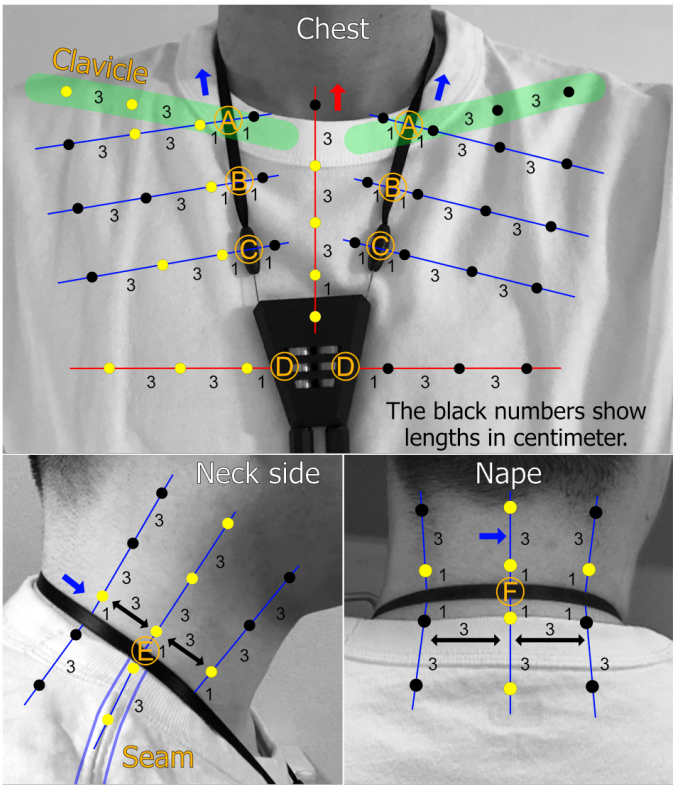

Fig. 3. Location of measurement points (black and yellow dots) measured in the pilot experiment described in Section V-A. The yellow points were selected using the pilot results. The red arrow indicates the direction of an accelerometer measured at points on the red line, and the blue arrows indicate that direction measured at points on the blue line (parallel to the ribbon). The orange circled letters are reference points in each row, coded as follows: A is the contact point between the ribbon and the clavicle; B is the midpoint between A and C; C is the center of the coupling; D is the midpoint of the housing; E is the point at which the ribbon crosses the shoulder seam line; F is the approximate center of the cervical vertebrae.

with amplitudes adjusted to consume 0.5, 1, and 2 W with one motor at a 20-Hz sine wave. Hereafter, the signal types are expressed as [frequency]-[power consumption]. For example, 20Hz-1W indicates an input signal with a frequency of 20 Hz and a voltage adjusted for one motor to consume 1 W. In the Hapbeat, the left and right motors wind and unwind the thread simultaneously. The vibration transmitted from the Hapbeat was measured with an analog triaxial accelerometer (NXP Semiconductors, MMA7361LC, using 6 G mode, module size of 10×10 mm, module mass of 0.4 g). Signals were recorded using an oscilloscope (Tektronix Inc, MDO4024C) at a sampling rate of 10 kHz and a recording time of one second. To evaluate the amplitude of the transmitted vibration, we used a_{RMS} in Eq. 1. To compare this amplitude with the predetermined reference amplitude, we used z_{RMS} in Eq. 1, which is the root-mean-square acceleration along the z-axis (perpendicular to the body surface).

$$a_{\mathrm{RMS}} = \sqrt{\frac{1}{N}\sum_{k=1}^{N}\left(|x_k-\mu_x|^2+|y_k-\mu_y|^2+|z_k-\mu_z|^2\right)} \tag{1}$$

TABLE II
FRICTION COEFFICIENT AND YOUNG'S MODULUS OF THE CLOTHING

Clothing	Direction	Friction Coefficient	Young's modulus (N/mm^2)
T-shirt	Vertical	0.188	573
	Horizontal	0.203	546
Dress shirt	Vertical	0.179	17.6
	Horizontal	0.178	11.0

$$z_{\mathrm{RMS}} = \sqrt{\frac{1}{N}\sum_{k=1}^{N}\left(|z_k - \mu_z|^2\right)} \tag{2}$$

$$\mu_x = \frac{1}{N}\sum_{k=1}^{N} x_k \tag{3}$$

where x_k, y_k, and z_k are sampled data for each axis and N is equal to 10×10^3 (points); Eq. (3) is of the same form for the y and z axes.

4) Clothing: In line with an everyday usage context, each subject wore a T-shirt or dress shirt and an undershirt. These clothes, made by Uniqlo Co., included a men's U Crew Neck Short-Sleeve T-Shirt (100% cotton), a men's Extra Fine Cotton Broadcloth Long-Sleeve Shirt (100% cotton), and an AIRism Micro Mesh V-Neck Short-Sleeve T-Shirt (comprising 83% nylon and 17% spandex). Subjects up to 170 cm tall wore the medium (M) sizes; taller subjects wore the large (L) sizes. The friction coefficients and Young's moduli of the T-shirt and dress shirt are shown in Table II. Friction coefficients were measured using a surface tester (Kato Tech Co Ltd, KES-FB4-A). For each material, a 20×20 cm fabric sample was prepared and tested six times using a weight of 400 g (for applying tension on the sample), and the average friction coefficient was calculated for each. Young's moduli were measured with a tensile tester (A&D Co Ltd, RTF-1250) Following the tensile testing protocol for fabrics in ISO Standard No. 13934-1:2013, five samples were cut along the straight grain and along the bias of the T-shirt, and three were cut from the dress shirt. Each sample was 50×300 mm, and the gripping interval during the test was 200 mm. Tests were conducted on each sample, and the average Young's modulus was calculated for each material.

5) Subjective evaluation: An experiment was conducted to verify the relationship between participants' subjective vibration perception and the measured acceleration magnitudes. Subjective perception was evaluated by asking participants to color-code measurement points in a figure (Fig. 3) with all explanatory numbers and letters omitted and all points initially colored black. The subjects were asked to color red where they felt the vibration clearly without needing to concentrate and blue where they felt the vibration subtly only when they concentrated on perceiving it. During this subjective experiment, vibration was continuously present on the subjects, and the subjects had no time limit to answer. Although we could not eliminate adaptation to vibrotactile stimuli, we accept this method as appropriate because the Hapbeat use case assumes that stimulating music vibration occurs for a long time; thus, we wanted to evaluate subjective perception after adaptation occurs. Furthermore, subjects could hear the audio noise from the Hapbeat, as mentioned in Section V-E1.

6) Procedure: First, the measurement points and an outline of the housing were marked on the subject's skin and clothing with a pen so that the Hapbeat could be restored to its initial location if misaligned during the experiment. Next, the accelerometer was attached to the measurement point with double-sided tape, with its x-axis parallel to the blue or red arrows (depending on location) in Fig. 3 and its z-axis perpendicular to the body surface. To maintain the attachment, an experimenter held the accelerometer cable 20 cm from the sensor part, taking care not to press the sensor on the body. At each point, measurements were taken once for input signals of 20Hz-0.5W, 20Hz-1W, and 20Hz-2W, and then the accelerometer was attached to another point. This procedure was repeated for all points in each region (the chest, neck side, and nape area).

Each subject stabilized their posture during the experiment by following instructions to sit on a chair with their upper body perpendicular to the seat surface, lightly press their back and head against the pole fixed directly behind the chair, look straight ahead, and exhale and hold their breath during the measurement. During the transition to the measurement of the next region, the subjective evaluations were carried out; then, breaks were taken as needed. This measurement procedure was conducted for all subjects once for each T-shirt and dress shirt.

7) Results: Results for the 20Hz-1W signal are shown in Fig. 4 as representative of the overall experiment. Note that the results outside of the pale orange area are for measurements conducted on clothing; that is, such results do not present transmitted vibration on the skin. The minimum mean values of z_{RMS} between subjects were 0.8 $\mathrm{m/s^2}$ at 20Hz-0.5W, 1.2 $\mathrm{m/s^2}$ at 20Hz-1W, and 1.7 $\mathrm{m/s^2}$ at 20Hz-2W (through both shirts).

8) Discussion of quantitative evaluation: The results show that z_{RMS} at all measurement points exceeds the reference amplitude of 0.32 $\mathrm{m/s^2}$ defined in Section I-A. Thus, the Hapbeat maintained the performance of our previously proposed driving principle and could transmit 20 Hz vibrations around the chest and neck with an intensity greater than airborne vibration from a loudspeaker playing a 130 dB sound. The value of a_{RMS} was highest at the neck side, which can be explained because a larger contact force, which increases frictional force, occurred on the neck side than on the chest, owing to the neck's greater curvature. The symmetric driving of the ribbon counteracted tangential forces on the nape. Contrary to expectations, the damping on the clavicle did not differ markedly from other locations. Because the ribbon did not vibrate the clavicle sufficiently and the relevant measurement point was on the clothing, the effect of bone conduction did not play into the system.

Comparing the results revealed that overall acceleration was greater for the dress shirts than for the T-shirts. This difference can be explained by the dress shirt having a larger Young's modulus and more rigidity than the T-shirt, thereby reducing the decay in vibration transmission. The measured acceleration of the housing was also greater for the dress shirt, which had a lower friction coefficient. We also observed that the

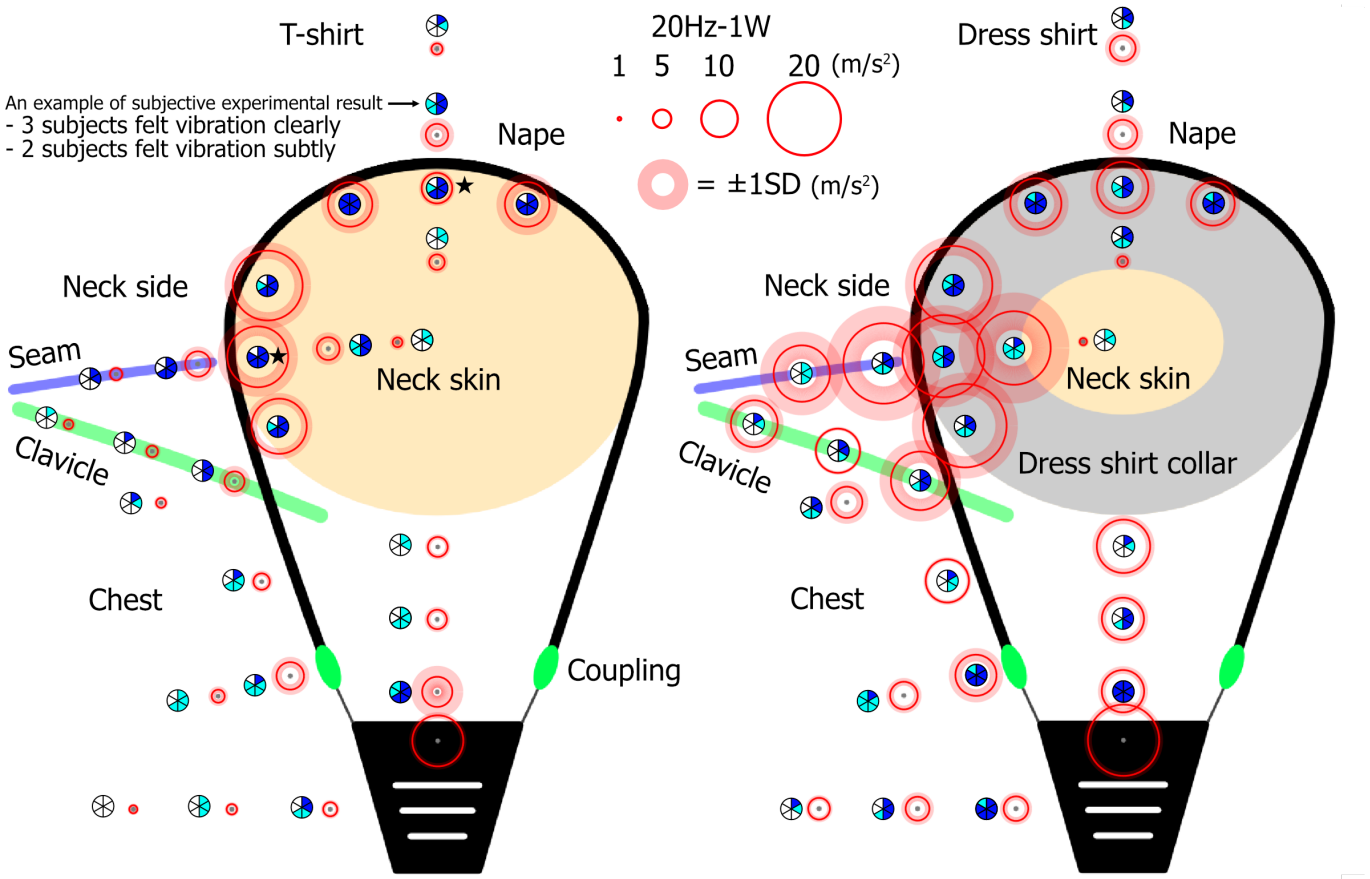

Fig. 4. Vibrations transmitted to the subjects (n = 6) and subjective perceptions. The solid red circles represent the magnitude of a_{RMS} values, and the red translucent area indicates one standard deviation (±SD). Results in the pale orange areas indicate measurements conducted on the skin, and those in other areas indicate measurements conducted on clothing (the gray area indicates the dress shirt's collar). The pie charts at or beside each point show the number of subjects who answered "clearly perceived" in deep blue and "slightly perceived" in light blue. The measurement points near the black stars are addressed in Section V-B.

soft and easily deformable T-shirt got caught on the housing, limiting movement. This phenomenon might also occur with other general vibrators attached to clothes. High variance was observed on the neck side area of the dress shirt, except near the ribbon. This could be due to the individual differences in wrinkling and tensions of the dress shirt fabric due to the subjects' differing body shapes (e.g., shoulder width and chest circumference).

9) Discussion of subjective evaluation: The subjective results (pie charts in Fig. 4) demonstrate that most subjects could perceive transmitted vibration near the housing and ribbon at the neck side and nape. Furthermore, more subjects perceived the vibration at the distal point (4 or 7 cm from the ribbon or housing) over the chest area with the dress shirt than with the T-shirt. This suggests that vibration of the clothing itself may enhance the user's perception of vibration intensity.

Although the accelerations were lower near the coupling and housing compared to the neck side and nape areas, at least the same number of subjects perceived the vibration near the coupling and housing. This may have occurred because the thicker shapes of the coupling and housing compared to the ribbon may have affected haptic perception. The auditory noise from the coupling and the housing might also have contributed to these perceptions (see Section V-E1). Subjects could hear the audio noise during the experiment, and this auditory stimulation might have affected their vibration perception [27], [28]. However, subjects could answer the vibration distribution even at the distal points that generated no auditory noise. This result indicates that the subjects could perceive the transmitted vibration to the extent that they could classify the distribution and strength of the vibration on the skin.

B. Evaluation of waveform fidelity

We obtained the frequency spectrum of the transmitted vibration via the fast Fourier transform method. The three axial components of the acceleration measurements at the neck side and nape (the measurement point near the black stars in Fig. 4) were combined into one principal value. The waveform was ascertained by detecting the periodic peaks to identify and extract the first two cycles.

1) Results: Of the results obtained, the waveforms and frequency spectra of cases featuring rich harmonic components (neck side of sub-2 and nape of sub-1) and a strong 20-Hz component (both sub-6) are shown in Fig. 5 as representative examples.

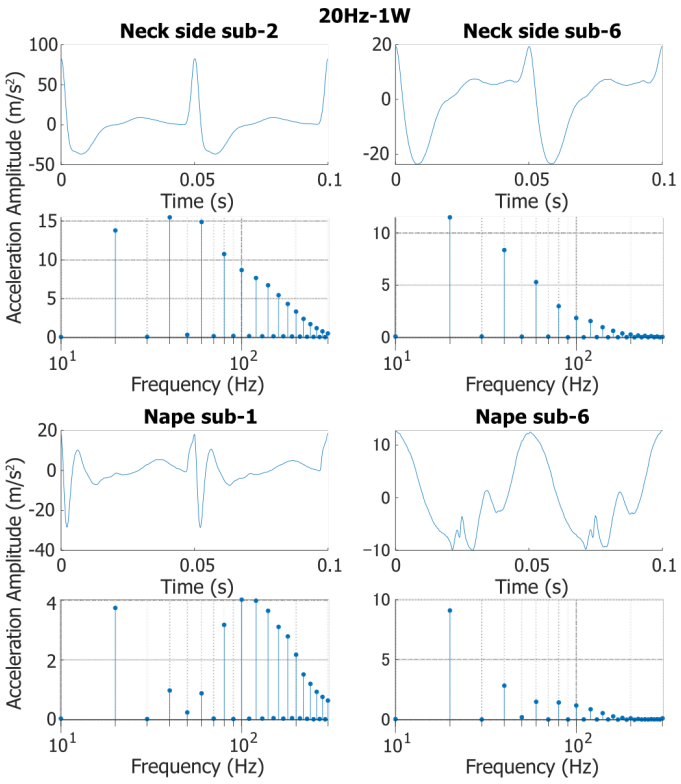

Fig. 5. Results of Fourier transform. The top graph in each pair shows acceleration along the principal axis from a 20-Hz sine wave input; the bottom graphs display results of the single-sided spectral analysis.

2) Discussion: In all cases, the transmitted vibrations comprise 20-Hz waves and harmonics. The transmission to the subject with a relatively high body fat percentage (i.e., sub-6) consisted mainly of 20-Hz vibrations, while for subjects with relatively low body fat percentages (i.e., sub-1 and sub-2), transmissions comprised mainly higher-frequency harmonics. Although the number of subjects in this experiment was insufficient to investigate any correlation with body fat, the difference in frequency composition of the transmitted vibration on the skin implies that vibration perception probably differs depending on the subject's body shape, body composition, and clothing.

C. Comparing power consumption with and without the mechanism

To evaluate the power-saving effect of the mechanism generating steady-state torque, we determined the power consumption of the Hapbeat motor when DC was applied to generate steady torque. This experiment required the Hapbeat motor to be removed from the housing, and the motor's bobbin only held the thread. The thread was wound three times around a single bobbin, and the free end was attached to a digital force gauge (Nidec-Shimpo Corporation, FPG-5) to measure the tension. A constant-voltage power supply device applied voltage to the motor and measured the current. The Hapbeat includes two motors and weighs 58.5 g, so the tension applied to each motor would be about 0.3 N under regular usage, which was our measurement target. The applied voltage was set to 0 V at the start of measurement and gradually increased less than 0.05 V per second. When the digital force gauge indicated 0.3 N, the current displayed on the power supply device was recorded (resolution of 0.01 A). We conducted the measurement five times.

1) Results: According to every measurement, the motor drew 0.32 A of DC to generate steady-state torque. Thus, using the steady-state torque mechanism in the Hapbeat would reduce the power consumption by 0.11 W per motor (calculated based on a motor resistance of 1.1 Ω and Ohm's law $P = RI^2 = 1.1\ \text{V} \times (0.32\ \text{A})^2 = 0.11\ \text{W}$).

D. Comparing the starting current

The static friction due to the implemented mechanism proposed in Section IV-B might prevent the thread from moving at the start of driving. To investigate the effect of the static friction, we measured the starting current values with the mechanism (Hapbeat case) and without (bare motor case). In both cases, only one motor was driven for measurement. For the bare motor case, the starting current was defined as the current when the shaft rotates from a resting state. In the case of the Hapbeat, the starting current was defined as the current value when the thread first moves from rest. The Hapbeat was suspended from a hook, with the accelerometer attached to the coupling on the driven motor side using double-sided tape. The accelerometer detected the first movement; its output was displayed on the oscilloscope. The same power supply device as described in Section V-C applied the voltage and measured the current.

1) Results: Over ten measurements, the starting currents of the bare motor case were all 0.01 A, while those of the Hapbeat averaged 0.55 A (standard deviation of 0.02 A). Derived from Ohm's law, the voltage applied to the motor terminal (1.1 Ω) at the first movement was 0.61 V in the Hapbeat case. This result indicates that the drive circuit needs to draw a current greater than 0.55 A and that the amplitude of the input signal should exceed 0.61 V to drive the Hapbeat from a static state. Note that the specific value of the starting current can vary among individuals; however, this paper does not discuss individual differences.

E. Audio noise from the Hapbeat

The audio noise from the Hapbeat was measured in a quiet room ($LAeq$ = 38 dB) with the subject (sub-6) wearing the T-shirt and the undershirt. A sound level meter (Shenzhen Wintact Electronics Co., Ltd, GM1356) was used for the measurements and placed at the same height as the housing, at 15 cm from the housing. The input signals were sine waves generated by the oscilloscope, with frequencies based on the E12 series (1.0, 1.2, 1.5, 1.8, 2.2, 2.7, 3.3, 3.9, 4.7, 5.6, 6.8, 8.2; these values were multiplied by 1, 10, and 100 for a total of 36 values ranging from 1–820 Hz), and the final signal was 1000 Hz. The signal amplitudes were adjusted so that each motor would consume 1 W. The audio noises from each signal were measured for 20 s with A-weighting, and the obtained mean SPL underwent background noise correction according

to ISO Standard No. 1996-1:1982. Measurements were conducted with and without a low-pass filter. Measurements with the filter were only taken for frequencies of 82 Hz or more (i.e., greater than the cutoff frequency of 72 Hz mentioned in Section IV-C). Input signal amplitude was the same in both cases.

1) Result: The measured SPLs are shown in Fig. 6. The sound types generated were as follows (judged qualitatively):

- At 1–3.3 Hz, a collision sound between the coupling and the housing and an abrasion sound between the housing and the clothing were produced.
- From 3.9–82 Hz, a clattering sound generated by the housing's up-and-down movement was recorded, along with a pattering sound when the ribbon was tensioned.
- From 100–1000 Hz, a magnetostriction sound (similar to the sound produced when the input signal is played through a speaker) was generated by the motor.

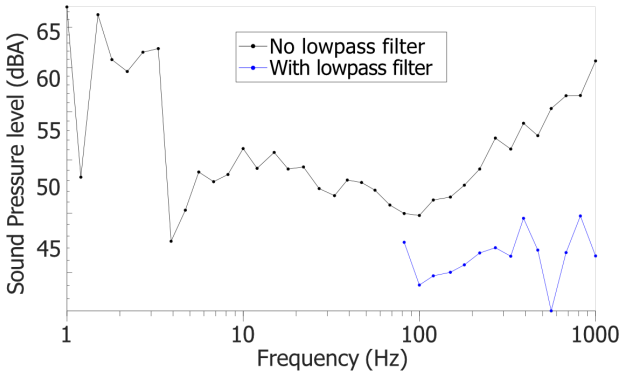

Fig. 6. Audio noise measurements.

2) Discussion: The measurements show that the audio noise from the Hapbeat was below 50 dBA with the low-pass filter. Considering that the SPL in public transport is around 70–80 dBA, the Hapbeat's audio noise is likely acceptable for use in such a situation. Applying the low-pass filter reduced information above 100 Hz, but the output of the Hapbeat was already weak in that range (as shown in the next experimental result, Fig. 8). Merchel *et al.* also supported using the low-pass filter: they showed that subjective perceptions of the auditory-tactile music experience are improved when music-induced vibrations are low-pass filtered [7]. Thus, the effect of applying the low-pass filter on the experience would be small or even positive. The audio noise in the 1–3.3 Hz range can be suppressed by modifying the materials and housing design; however, this is likely not necessary because music generally does not draw on this frequency band.

In terms of effect on the Hapbeat user, audio noise from the housing is unimportant because the music sound and headphones or earphones mask the noise. This experiment could not evaluate audio noise from bone conduction. The perceptibility of such audio noise must be verified, but we assume that it has no adverse effect on the experience, based on the study of Sakuragi *et al.* The authors showed that presenting music vibrations on the clavicle, which is more likely to produce bone conduction noise than the Hapbeat approach, had a positive effect on the music listening experience [18].

F. Frequency response of the Hapbeat

We measured the frequency response of the Hapbeat with a reproducible method using a mannequin made from a public three-dimensional (3D) model and a gel sheet to represent human skin. The experimental arrangement is shown in Fig. 7(c)–(f), and the details are as follows. The mannequin 3D model was "haf020.obj" from the 2003 AIST/HQL Human Body Size and Shape Database [**?**]. The model was divided into sections as shown in Fig. 7(a) and (b), and each section was 3D-printed (using Zortrax, Z-PLA Pro material, laminate thickness of 0.29 mm and infill 10% hexagonal). The printed parts were joined with double-sided tape. The gel sheet (Exseal Co., Ltd., H0-3K) was sticky on one side and smooth on the other. The smooth side was covered with a urethane film. A 50×500 mm piece was attached around the neck of the mannequin, and a 230×290 mm piece was attached to the chest part.

Four measurements were taken to obtain accelerations on the chest, housing, nape, and neck side. To measure up to 1000 Hz, we used another accelerometer with a wide frequency bandwidth (Analog Devices, Inc., ADXL354C, module size of 18×12.7 mm, module mass of 1 g). The accelerometer was applied directly onto the location shown in Fig. 7(c)–(f) using double-sided tape, and the sensor cable, which was 20 cm away from the sensor module, was taped to the mannequin. The input signal was the same as used in Section V-E, and the output was recorded with the oscilloscope with a sampling rate of 1 kHz for 1–8.2 Hz inputs and 10 kHz for inputs over 10 Hz.

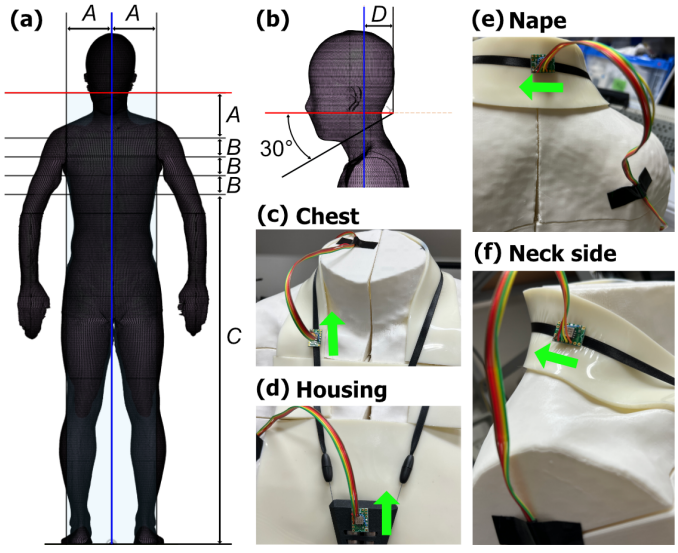

Fig. 7. Schematic of the dimensions of the 3D-printed mannequin (a)–(b) and measurement conditions (c)–(f). The letters in (a) and (b) indicate the dimensions: A = 150 mm, B = 62.5 mm, C = 1,100 mm, and D = 70 mm. The red and blue lines in (a) correspond to those in (b). The green arrows in (c)–(f) indicate the direction of the accelerometer's x-axis.

1) Results: Results are shown in Fig. 8. The a_{RMS} was over 10 $\mathrm{m/s^2}$ when the frequency ranges were 2.2–470 Hz for the position at the chest, 10–100 Hz at the housing, and 2.2–270 Hz at the neck side, while the a_{RMS} measured at the nape never exceeded 10 $\mathrm{m/s^2}$.

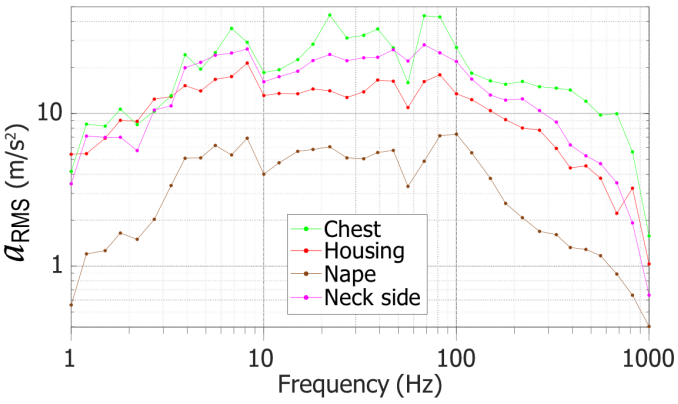

Fig. 8. Frequency response of the Hapbeat on the mannequin.

G. Response time of the Hapbeat

To determine the response time of the Hapbeat, the change in thread tension was measured with a force sensor (PCB Piezotronics, Inc., 208C01) when a step voltage was applied to the motor. The Hapbeat hung on a 3D-printed hook, and the hook was attached to the sensor tip. Step voltage was applied by turning on a battery box that contained two 1.2-V AA cells in series. To normalize the measured data, the values before the application of step voltages were set to zero, and the steady-state average after input was set to one. The steady-state criterion was defined as voltage drift within 0.1 V per second. The duration of interest was from the normalized input voltage exceeding 0.9 V to the normalized tension value exceeding 0.9 N.

1) Results: The average delay over the ten trials was 2.74 ms, with a maximum of 3.00 ms.

VI. General Discussion and Limitations

The experimental results demonstrate that the Hapbeat is a successful haptic device, employing our previously proposed driving principle, that can be used in everyday travel situations, such as commuting or using public transportation. The Hapbeat is easily wearable (can be put on in less than five seconds) and battery-powered, which makes it convenient, and its audio noise is less than 50 dBA with a low-pass filter.

In addition, the Hapbeat can effectively transmit low-frequency vibration. It can transmit 20 Hz vibrations over the chest and neck with an intensity greater than airborne vibration from a loudspeaker playing a 130 dB sound. Furthermore, no significant attenuation occurs up to 470 Hz, and the response speed is 2.74 $\mathrm{m/s^2}$, which is comparable to that of a coreless motor or linear vibrator [21]. Thus, the Hapbeat covers a wide range of low music frequencies and responds to instantaneous input signals, such as drum sounds, with little delay, making it a high-performing haptic device for music listening.

However, we cannot say definitively that the Hapbeat can reproduce actual musical vibrations faithfully. The transmitted vibrations exceeded 10 $\mathrm{m/s^2}$ in a_{RMS} near the ribbon, which is much greater than the reference amplitude. Vibrations in this range are thus perceived more strongly near the ribbon, differing from the sensory distribution of a live music experience. Additionally, while the reference value is useful for comparison with airborne vibration, attempts to reproduce a realistic music experience should also consider structure-borne vibration and the sensation caused by the pressure difference inside and outside the human body. Thus, we cannot directly compare the experience of using the Hapbeat with that of being in a nightclub. Nevertheless, this vibration perception may still contribute positively to the intensity and enjoyment of a music experience. Hence, the relationship between the magnitude and distribution of transmitted vibration and the subjective evaluation of musical haptic experience should be investigated.

The low-frequency vibration outputs contained strong harmonics due to poor reproduction of the input signal (Fig. 5). Because the Hapbeat is suspended, the acceleration of the housing cannot exceed the housing's gravitational acceleration while the motor unwinds and loosens the thread. Thus, the Hapbeat sometimes discards the thread-unwinding part of input signals while maintaining the thread-winding part. Furthermore, as indicated in Section V-D, the internal friction between the thread or rubber cord and the Teflon tubes impedes thread movement in cases of weak input voltage, and overcoming that friction threshold leads to a rapid, intense actuation when the input voltage exceeds a certain value. These phenomena cause the Hapbeat to reflect the input signal faithfully only under the following conditions: when the motor output torque exceeds internal static friction and when the acceleration of the housing is less than the gravitational acceleration of the housing (in thread-unwinding movements). These mechanical characteristics introduce harmonics into the Hapbeat's output, as shown in Fig. 5. The extent to which users can perceive these harmonics of transmitted vibrations much larger than the threshold in actual usage is unknown, and this needs to be investigated.

Measuring the transmitted vibration directly on the skin under the clothing was not possible. We tried to attach the accelerometer directly to the skin by placing it under the clothing or cutting a hole in the clothing the size of the accelerometer and attaching it to the exposed skin. However, we decided against this approach because the transmission characteristic from the ribbon to the skin differs from the actual clothing condition. Therefore, we cannot claim from the quantitative results shown in Fig. 4 that vibrations were transmitted to the skin under the clothing, but the subjective results shown in Fig. 4 indicate that noticeable vibration was transmitted successfully for the following reasons: some subjects could perceive vibrations at the distal points, and results varied depending on clothing type, indicating that subjects felt vibration from the vibrating clothing. Although establishing a method for measuring vibration transmitted to the skin surface through clothing is beyond this paper's scope, further investigation is needed to observe such vibration

accurately.

VII. Conclusion

This paper presents a design and implementation method of a necklace-type haptic device that uses our previously proposed driving principle and is practical in for everyday travel situations, such as commuting or riding on public transport. Experiments showed that the Hapbeat, which is compact, lightweight, and easy to wear, can transmit low-frequency vibrations over a wide skin area. The proposed method will be helpful for developing a convenient device capable of transmitting low-frequency vibrations, a goal that has been difficult to achieve with conventional haptic devices. Although this paper focuses on the necklace-type device and assumes everyday usability, the method can also be applied to other wearable haptic devices, such as belt- or wristband-type devices. We hope that our proposal contributes to enhance haptic devices' performance and usability and creates new ways to use haptic devices for entertainment, ultimately widening their range of applications.

Acknowledgment

This work was supported by JSPS KAKENHI Grant Numbers JP17H01774, JP20H04220.

References

[1] M. Karam, C. Branje, G. Nespoli, N. Thompson, F. A. Russo, and D. I. Fels, "The emoti-chair: an interactive tactile music exhibit," in *CHI'10 Extended Abstracts on Human Factors in Computing Systems*, 2010, pp. 3069–3074.

[2] Y. Konishi, N. Hanamitsu, B. Outram, K. Minamizawa, T. Mizuguchi, and A. Sato, "Synesthesia suit: the full body immersive experience," in *ACM SIGGRAPH 2016 VR Village*, 2016, pp. 1–1.

[3] "SUBPAC," https://subpac.com/, accessed: 2022-02-14.

[4] "woojer," https://www.woojer.com/, accessed: 2022-02-14.

[5] "bhaptics," https://www.bhaptics.com/, accessed: 2022-02-14.

[6] M. J. Hove, S. A. Martinez, and J. Stupacher, "Feel the bass: Music presented to tactile and auditory modalities increases aesthetic appreciation and body movement." *Journal of Experimental Psychology: General*, vol. 149, no. 6, p. 1137, 2020.

[7] S. Merchel and M. E. Altinsoy, "Auditory-tactile experience of music," in *Musical Haptics*. Springer, Cham, 2018, pp. 123–148.

[8] R. T. Verrillo, "Vibration sensation in humans," *Music Perception*, vol. 9, no. 3, pp. 281–302, 1992.

[9] Y. Yamazaki, H. Mitake, and S. Hasegawa, "Tension-based wearable vibroacoustic device for music appreciation," in *International conference on human haptic sensing and touch enabled computer applications*. Springer, 2016, pp. 273–283.

[10] "What dB level can you be exposed to in a Nightclub and how dangerous is it for your hearing?" https://www.instrumentchoice.com.au/what-db-level-can-you-be-exposed-to-in-a-nightclub-and-how-dangerous-is-it-for-your-hearing, accessed: 2022-02-14.

[11] Y. Takahashi, K. Kanada, and Y. Yonekawa, "Some characteristics of human body surface vibration induced by low frequency noise," *Journal of Low Frequency Noise, Vibration and Active Control*, vol. 21, no. 1, pp. 9–19, 2002.

[12] K. O. Sofia and L. Jones, "Mechanical and psychophysical studies of surface wave propagation during vibrotactile stimulation," *IEEE transactions on haptics*, vol. 6, no. 3, pp. 320–329, 2013.

[13] P. Lemmens, F. Crompvoets, D. Brokken, J. Van Den Eerenbeemd, and G.-J. de Vries, "A body-conforming tactile jacket to enrich movie viewing," in *World Haptics 2009-Third Joint EuroHaptics conference and Symposium on Haptic Interfaces for Virtual Environment and Teleoperator Systems*. IEEE, 2009, pp. 7–12.

[14] Y. Chandra, B. Tag, R. L. Peiris, and K. Minamizawa, "Preliminary investigation of across-body vibrotactile pattern for the design of affective furniture," in *2020 IEEE Haptics Symposium (HAPTICS)*. IEEE, 2020, pp. 671–676.

[15] A. Israr, S.-C. Kim, J. Stec, and I. Poupyrev, "Surround haptics: tactile feedback for immersive gaming experiences," in *CHI'12 Extended Abstracts on Human Factors in Computing Systems*, 2012, pp. 1087–1090.

[16] J. H. Hogema, S. C. De Vries, J. B. F. Van Erp, and R. J. Kiefer, "A tactile seat for direction coding in car driving: Field evaluation," *IEEE Transactions on Haptics*, vol. 2, no. 4, pp. 181–188, Oct 2009.

[17] S. Nanayakkara, E. Taylor, L. Wyse, and S. H. Ong, "An enhanced musical experience for the deaf: design and evaluation of a music display and a haptic chair," in *Proceedings of the SIGCHI Conference on Human Factors in Computing Systems*, 2009, pp. 337–346.

[18] R. Sakuragi, S. Ikeno, R. Okazaki, and H. Kajimoto, "Collarbeat: Whole body vibrotactile presentation via the collarbone to enrich music listening experience." in *ICAT-EGVE*. Citeseer, 2015, pp. 141–146.

[19] Y. Kurihara, M. Koge, R. Okazaki, and H. Kajimoto, "Large-area tactile display using vibration transmission of jammed particles," in *2014 IEEE Haptics Symposium (HAPTICS)*. IEEE, 2014, pp. 313–318.

[20] A. Withana, S. Koyama, D. Saakes, K. Minamizawa, M. Inami, and S. Nanayakkara, "Rippletouch: initial exploration of a wave resonant based full body haptic interface," in *Proceedings of the 6th Augmented Human International Conference*, 2015, pp. 61–68.

[21] V. Yem, R. Okazaki, and H. Kajimoto, "Vibrotactile and pseudo force presentation using motor rotational acceleration," in *2016 IEEE Haptics Symposium (HAPTICS)*. IEEE, 2016, pp. 47–51.

[22] R. Gourishetti and K. J. Kuchenbecker, "Evaluation of vibrotactile output from a rotating motor actuator," *IEEE Transactions on Haptics*, vol. 15, no. 1, pp. 39–44, 2021.

[23] K. Minamizawa, S. Fukamachi, H. Kajimoto, N. Kawakami, and S. Tachi, "Gravity grabber: wearable haptic display to present virtual mass sensation," in *ACM SIGGRAPH 2007 emerging technologies*, 2007, pp. 8–es.

[24] T. Nakamura, V. Yem, and H. Kajimoto, "Hapbelt: haptic display for presenting vibrotactile and force sense using belt-winding mechanism," in *SIGGRAPH Asia 2017 Emerging Technologies*, 2017, pp. 1–2.

[25] L. Yan, Z. Chen, Y. Zou, X. He, C. Cai, K. Yu, and X. Zhu, "Field study of the interior noise and vibration of a metro vehicle running on a viaduct: A case study in guangzhou," *International journal of environmental research and public health*, vol. 17, no. 8, p. 2807, 2020.

[26] S. Hapuarachchi, D. Jayaratna, C. Kalansuriya, and A. Pannila, "Noise level survery inside the inter provincial buses in sri lanka," in *Proceedings of the Technical Sessions*, vol. 23, 2007, pp. 35–40.

[27] S. Guest, C. Catmur, D. Lloyd, and C. Spence, "Audiotactile interactions in roughness perception," *Experimental Brain Research*, vol. 146, no. 2, pp. 161–171, 2002.

[28] C. Spence and A. Gallace, "Recent developments in the study of tactile attention." *Canadian Journal of Experimental Psychology/Revue canadienne de psychologie expérimentale*, vol. 61, no. 3, p. 196, 2007.

Yusuke Yamazaki received the M.S. degree in information and communications engineering from Tokyo Institute of Technology in 2017. He established Hapbeat LLC. in 2017 to commercialize haptic device using invented vibration mechanism. His research interest is the popularization and social implementation of haptic technology relating to XR technologies and entertainment.

Hironori Mitake received the D.Eng. degree in computational intelligence and systems from the Tokyo Institute of Technology, Tokyo, Japan. He has been an Associte Professor with the Meiji University since 2022 and was previously an Assistant Professor with the Tokyo Institute of Technology since 2011. His domain of research includes virtual creature, embodied agent, haptic interaction, entertainment computing, and virtual reality.

Shoichi Hasegawa received the D.Eng. degree in computational intelligence and systems from the Tokyo Institute of Technology, Tokyo, Japan. He has been an Associate Professor with the Tokyo Institute of Technology since 2010 and was previously an Associate Professor with the University of Electro Communications. His domain of research includes haptic renderings, realtime simulations, interactive characters, soft and entertainment robotics, and virtual reality.